Allyl Isothiocyanate Modulates Antioxidant and Detoxification Systems in *Coptotermes formosanus*

Wanyan Jiang , Lijun Cai , Tianyi Yang , Jiafu Zhang , Qi Zhao , Meixiang Wu *

Posted Date: 22 May 2026

doi: 10.20944/preprints202605.1541.v1

Keywords: allyl isothiocyanate; acetylcholinesterase; antioxidant enzymes; detoxification enzymes; molecular docking

 doi:10.20944/preprints202605.1541.v1

Article

Allyl Isothiocyanate Modulates Antioxidant and Detoxification Systems in *Coptotermes formosanus*

Wanyan Jiang [1,2], Lijun Cai [1,3], Tianyi Yang [1], Jiafu Zhang [1], Qi Zhao [4] and Meixiang Wu [1,2,*]

[1] State Key Laboratory of Agricultural and Forestry Biosecurity, College of Plant Protection, Fujian Agriculture and Forestry University, Fuzhou 350002, China
[2] Biological Control Research Institute, Fujian Agriculture and Forestry University, Fuzhou 350002, China
[3] Institute of Applied Ecology, Fujian Agriculture and Forestry University, Fuzhou 350002, China
[4] Fuzhou Greening Management Office, Fuzhou 350003, China
* Correspondence: wuivy2000@126.com

Simple Summary

Coptotermes formosanus is a destructive insect pest that harms landscape plants and wooden structures, causing severe economic losses. At present, the control of termites mainly relies on chemical pesticides, causing substantial environmental problems. In this study, we measured the active and relative gene expression of antioxidant enzymes, detoxification enzymes and neural enzymes when *C. formosanus* are exposed to AITC. We found that AITC can induce the activities of these enzymes but the expression of related genes exhibits different levels. Molecular docking results showed that AITC binds well to all the above enzymes. These results indicate that AITC induces both enzymatic and transcriptional changes in *C. formosanus*, and could be developed into an environmentally friendly agent for termite control.

Abstract

The Formosan subterranean termite, *Coptotermes formosanus*, is a globally distributed species that feeds on lignocellulose and causes substantial economic losses annually. Current control strategy heavily relies on chemical pesticides, raising concerns about environmental impacts associated with their overuse. Allyl isothiocyanate (AITC), a plant-derived pesticide, has demonstrated significant insecticidal activity. However, its effects on key physiological and biochemical systems in *C. formosanus* remain poorly understood. In particular, its impact on antioxidant enzymes, including superoxide dismutase (SOD), catalase (CAT), and peroxidase (POD), detoxification enzymes such as carboxylesterase (CarE), glutathione S-transferase (GST), and neural enzymes (e.g., acetylcholinesterase, AChE) has not been systematically investigated. Transcriptome data were used to predict coding sequences (CDSs) of antioxidant, detoxification, and neural enzymes, followed by phylogenetic analysis. *C. formosanus* was treated with AITC at LC_{50} for 24 h, and enzyme activities and gene expression levels were assessed. Molecular docking was performed to evaluate interactions between AITC and the five enzymes. AITC exposure significantly increased the activities of all six enzymes. Gene expression analysis revealed differential regulation across enzyme families, with notable upregulation of AChE and several CarE, SOD, POD, and GST genes. Docking analysis indicated favorable binding affinity to target enzymes (binding energy < -1.2 kcal/mol). These findings suggest that AITC induces coordinated enzymatic and transcriptional responses in *C. formosanus*, providing insight into its mode of action and supporting its potential as a botanical termiticide with low environmental impact.

Keywords: allyl isothiocyanate; acetylcholinesterase; antioxidant enzymes; detoxification enzymes; molecular docking

 doi:10.20944/preprints202605.1541.v1

1. Introduction

Coptotermes formosanus (Blattodea: Heterotermitidae) is a eusocial insect species with a remarkable capacity for efficient lignocellulose degradation and utilization [1,2]. It exhibits strong dispersal ability and environmental adaptability, causing severe damage to wooden structures and resulting in substantial economic losses annually [3]. Moreover, its potential distribution is projected to expand under ongoing climate change [4]. Current termite control strategies rely heavily on chemical pesticides, including pyrethroids, neonicotinoids, organofluorines, and insect growth regulators [5]. However, the widespread application of these chemicals in buildings and soil raises concerns about environmental contamination and risks to human health.

Botanical insecticides have garnered increasing attention in recent years due to their biodegradability, diverse modes of action, and reduced risk of resistance development [6]. Numerous plant-derived compounds, particularly essential oils and their constituents, exhibit strong insecticidal and repellent activities against termite species. For example, essential oils from *Cunninghamia konishii* and *Cryptomeria japonica*, as well as their major components, have demonstrated significant toxicity to *Coptotermes formosanus* [7,8]. Similarly, compounds such as 1,8-cineole from *Eucalyptus camaldulensis* show fumigant toxicity and can inhibit acetylcholinesterase activity, suggesting neurotoxic effects [9]. In addition to essential oils, isothiocyanates represent another important class of plant-derived bioactive compounds. Allyl isothiocyanate (AITC), a secondary metabolite produced by cruciferous plants upon tissue damage, has demonstrated potent insecticidal activity against a wide range of insect pests [10–13]. Previous studies have shown that AITC can alter detoxification and antioxidant enzyme activities and may target key metabolic pathways, such as cytochrome c oxidase [14]. However, the underlying mechanisms remain insufficiently understood, particularly in termites.

In insects, antioxidant enzymes including superoxide dismutase (SOD), catalase (CAT), and peroxidase (POD) play essential roles in mitigating oxidative stress by scavenging reactive oxygen species generated under environmental and chemical challenges. These enzymes are critical for maintaining cellular homeostasis and protecting tissues from oxidative damage [15–17,47]. In parallel, detoxification enzymes such as cytochrome P450s, carboxylesterases (CarEs) and glutathione S-transferases (GSTs) are involved in the metabolism and elimination of xenobiotic compounds, including insecticides, thereby contributing to insect survival and tolerance to toxic exposure [18–21]. Acetylcholinesterase (AChE) terminates cholinergic neurotransmission by hydrolyzing acetylcholine (ACh), thereby restoring synaptic function. As a member of the clade of esterases, AChE plays a central role in neural transmission and is a well-established target of insecticides that disrupt nervous system activity [20, 22]. Given the central roles of antioxidant enzymes, detoxification systems, and AChE in maintaining physiological homeostasis and mediating responses to toxic exposure, these pathways may represent key targets of AITC action.

Molecular docking is a computational approach that identifies potential bioactive compounds by screening target protein models. After quality evaluation, these templates are computationally docked with ligand molecules and binding energies are calculated to screen for substances likely to regulate biological behavior [23–24]. With the rapid development of bioinformatics, molecular docking has been widely applied in pest control research. For instance, molecular docking results indicated that caryophyllene oxide, a major component of citronella essential oil, exhibits inhibitory potential against insect α-amylase [25]. Additionally, molecular docking suggests that the bioactivity of turmeric essential oil against pests may be related to its interaction with AChE [26].

Among molecular docking tools, CB-Dock enables blind docking of protein-ligand complexes by integrating cavity detection, automated docking, and homologous template fitting, effectively predicting the three-dimensional structures of proteins and ligands along with their binding sites and affinities [27]. Its upgraded version, CB-Dock2, further incorporates template-based docking strategies, significantly improving the accuracy of binding site identification and binding pose prediction. Benchmark tests demonstrated that CB-Dock2 achieves a success rate of approximately

 doi:10.20944/preprints202605.1541.v1

85% in predicting binding poses (RMSD < 2.0 Å), outperforming the original CB-Dock and most mainstream blind docking tools [28].

Our previous study determined the fumigation toxicity of AITC against *C. formosanus*, with an LC_{50} of 435.993 μL/L under laboratory conditions [29]. In this study, the effects of AITC at the LC_{50} level on the activities and gene expression of antioxidant enzymes, detoxification enzymes, and acetylcholinesterase (AChE) in *C. formosanus* were investigated. In addition, molecular docking was performed to evaluate the potential interactions between AITC and these enzymes, including binding sites, binding affinities, and key amino acid residues. This study aims to elucidate the biochemical and molecular responses of *C. formosanus* to AITC exposure and to provide insights into its potential mode of action, thereby contributing to the development of sustainable termite control strategies.

2. Materials and Methods

2.1. Insects Collection and Maintenance

A colony of *C. formosanus* was collected from Huazhou City (Guangdong Province, China) (21.66°N, 110.64°E) in February 2024. The colony was subsequently maintained in the laboratory for one week in a plastic box (18 cm × 10 cm × 10 cm) at 28 ± 1 ◦C, 75 ± 5% relative humidity (RH) and a 24:0 h (dark: light) before conducting enzyme activity and gene expression assays. All experiments were conducted in an environmental chamber (PRX-350B, Plant Instrument Co., Ltd., Ningbo, China). Water and filter paper were utilized as a food source.

2.2. Exposure of C. formosanus to AITC at LC_{50}

A total of 1,200 worker termites (*C. formosanus*) were randomly divided into six groups, with three groups serving as controls (CK: C1, C2, C3) and the other three as AITC-treated groups (AT: A1, A2, A3). The AITC (99.99%) used was purchased from Yeyuan Biotechnology Co., Ltd (Shanghai, China). n-hexane (99.99%, Macklin Biochemical Co., Ltd., Shanghai, China) was served as the solvent for AITC dilution and the control treatment. Termites in the AT groups were exposed to AITC at LC_{50} concentration (435.993 μL/L), whereas those in the CK groups received an equal volume of n-hexane. A PRX-350B Intelligent Artificial Climate Chamber (Plant Instrument Co., Ltd., Ningbo, China) was used for termite rearing. After 24 h of exposure, surviving individuals were immediately frozen in liquid nitrogen and stored at -80 °C for subsequent enzyme activity assays and gene expression analysis.

2.3. Enzyme Activity Assays

Surviving worker termites from each group (C1, C2, C3, A1, A2, A3) after 24-hour treatment were selected for enzyme activity determination. For each replicate, 150 termites were pooled, weighed, and homogenized in ice-cold extraction buffer (e.g., [provide composition, such as 0.1 M phosphate buffer, pH 7.0, containing 0.1 mM EDTA]) according to the manufacturer's instructions. The homogenate was centrifuged at 8,000 × g for 10 min at 4 °C, and the supernatant was collected as the crude enzyme extract and kept on ice until analysis. Enzyme activity assay kits for acetylcholinesterase (AChE [ZC-S0384]), carboxylesterase (CarE [ZC-S0387]), glutathione S-transferase (GST [ZC-S0333]), catalase (CAT [ZC-S0351]), peroxidase (POD [ZC-S0352]), and superoxide dismutase (SOD [ZC-S0350]) were supplied by ZCIBIO Technology Co., Ltd (Shanghai, China). Total protein concentration in the enzyme extracts was determined using the Bradford method, and enzyme activities were normalized to protein content.

Enzyme activities were determined using an MD-SpectraMax 190 multi-mode microplate reader (Molecular Devices Co., Ltd., Shanghai, China) according to the manufacturers' instructions for the corresponding assay kits. Absorbance was recorded at 450 nm for SOD and CarE, 470 nm for POD, 240 nm for CAT, 340 nm for GST, and 412 nm for AChE. Enzyme activity units were defined according to the kit protocols as follows: SOD, the amount of enzyme causing 50% inhibition in the xanthine oxidase-coupled reaction; POD, the amount causing a 0.005 absorbance change per minute;

 doi:10.20944/preprints202605.1541.v1

CAT, the amount catalyzing the degradation of 1 nmol H_2O_2 per minute; GST, the amount catalyzing the conjugation of 1 μmol 1-chloro-2,4-dinitrobenzene (CDNB) with glutathione (GSH) per minute; CarE, the amount resulting in an absorbance increase of 1.0 per minute; and AChE, the amount catalyzing the formation of 1 nmol 5-thio-2-nitrobenzoic acid (TNB) per minute. Enzyme activities were expressed as U/g fresh weight or nmol/min/g (AChE).

2.4. CDS Identification and Phylogenetic Analysis

We predicted CDS of the transcriptome data using a homology-based approach [29]. Transcript sequences were first aligned sequentially against the Swiss-Prot and NR protein databases using BLAST-X [30], and coding regions were inferred based on the best significant alignments. Based on the predicted CDSs, sequences corresponding to antioxidant and detoxification enzymes, including SOD, CAT, POD, CarE, GST, and AChE were identified and extracted. These sequences were subsequently used for phylogenetic analysis. The predicted CDSs were translated to amino acid sequences. Homologous protein sequences were retrieved from the NCBI database and used for phylogenetic tree construction. The accession numbers and full names of all sequences are provided in Supplementary Table 1. Phylogenetic tree analysis was performed using MEGA 11 software [31]. Amino acid sequences were aligned, and phylogenetic trees were constructed using the Neighbor-Joining method [32]. The robustness of the tree topology was evaluated using bootstrap analysis with 1000 replicates [33], and bootstrap support values are indicated at the nodes. Evolutionary distances were computed using the p-distance method [34]. All other parameters were set to default values.

2.5. RNA Isolation, cDNA Synthesis, and RT-qPCR

Surviving *C. formosanus* workers from each group after 24-hour AITC exposure were collected for RNA extraction. For each sample, approximately 0.1 g of termite tissue was ground into fine powder in liquid nitrogen. Total RNA was extracted using a commercial RNA extraction kit (Herui Biotechnology Co., Ltd., Fuzhou, China) according to the manufacturer's instructions. RNA concentration was measured using a BioDrop μLite Ultra low volume spectrometer (BioDrop Ltd., Cambridge, UK). cDNA was synthesized using OneStep gDNA Removal and reverse transcription kit (Herui Biotechnology Co., Ltd., Fuzhou, China) according to the manufacturer's instructions. Reverse transcription was performed in a Thermal Cycler (Mona Biotechnology Co., Ltd., Suzhou, China) using total RNA as the template under the following conditions: 42 °C for 15 min, followed by 85 °C for 10 sec. The synthesized cDNA was stored at -20 °C for subsequent RT-qPCR analysis. Based on the predicted CDS and phylogenetic analysis, specific primers were designed for AChE, CarE, GST, CAT, POD, and SOD. The 18S rRNA gene was used as the internal reference gene [35] (Table S2).

RT-qPCR was performed on a Gentier 96R Automated Medical PCR Analysis System (Tianlong Technology Co., Ltd., Xian, China) using HRbio qPCR SYBR Green Master Mix (No Rox) (Herui Biotechnology Co., Ltd., Fuzhou, China) following the manufacturer's protocol. The amplification program consisted of an initial denaturation at 95 °C for 5 min, followed by 40 cycles of denaturation at 95 °C for 10 s, annealing at 58 °C for 20 s, and extension at 72 °C for 20 s. A melt curve analysis was subsequently performed at 95 °C for 1 min, 60 °C for 15 s, and 98 °C for 5 s. The total reaction volume was 20 μL and consisted of 1 μL of 0.4 μL cDNA, 10 μL of qRT-PCR SYBR Green Master Mix, 0.4 μL forward primers, 0.4 μL reverse primers (Table S1), and 8.8 μL ddH_2O. Relative gene expression levels were calculated using the $2^{-\Delta\Delta Ct}$ method [36]. Three biological replicates were performed, each with three technical replicates.

2.6. Molecular Docking

Amino acid sequences were translated from the predicted CDSs using the standard codon table, excluding sequences containing stop codons or incomplete open reading frames. The translated sequences were aligned with homologous reference sequences retrieved from the NCBI GenBank

 doi:10.20944/preprints202605.1541.v1

database using ClustalW with default parameters. For each target enzyme family, the sequence most significantly induced by AITC was selected as the representative for molecular docking. The selected sequences were submitted to the SWISS-MODEL server (https://swissmodel.expasy.org/) to predict three-dimensional (3D) protein structures using homology modeling with templates from the Protein Data Bank (PDB)[37]. Meanwhile, the 3D structure of AITC was downloaded from the PubChem (https://pubchem.ncbi.nlm.nih.gov/) database in PDB format. The predicted protein models and the AITC structure were uploaded to the CB-Dock2 server (http://clab.labshare.cn/cb-dock2/) for molecular docking, with automatic detection of binding pockets and default parameters. The docking conformation with the lowest binding energy was selected as the optimal binding mode for subsequent analysis.

2.7. Statistical Analysis

Data on enzyme activities and relative gene expression levels among different groups were analyzed using GraphPad Prism 8.0.2 software (GraphPad Software, USA). Differences between groups were assessed using Student's *t* tests or nonparametric tests when assumptions of normality were not met. Statistical significance was set at $P < 0.05$.

3. Results

3.1. AITC Exposure at LC_{50} Enhances Acetylcholinesterase, Detoxification, and Antioxidant Enzyme Activities in C. formosanus

To elucidate the effects of AITC at LC_{50} on antioxidant, detoxification, and acetylcholinesterase activities in *C. formosanus*, these enzyme activities were measured in termites exposed to n-hexane (control, CK) or LC_{50} of AITC (AT). Relative to the control, treatment with 435.993 μL/L AITC significantly increased the activities of all enzymes tested, including AChE, CarE, GST, CAT, POD, and SOD. Specifically, the antioxidants CAT, POD, and SOD were 43%, 31%, and 40% higher than those in the control group, respectively. The activities of detoxification enzymes GST and CarE increased by 64% and 59%, respectively, compared with the control. Acetylcholinesterase (AChE) activity was 44% higher than that of the control (Fig. 1).

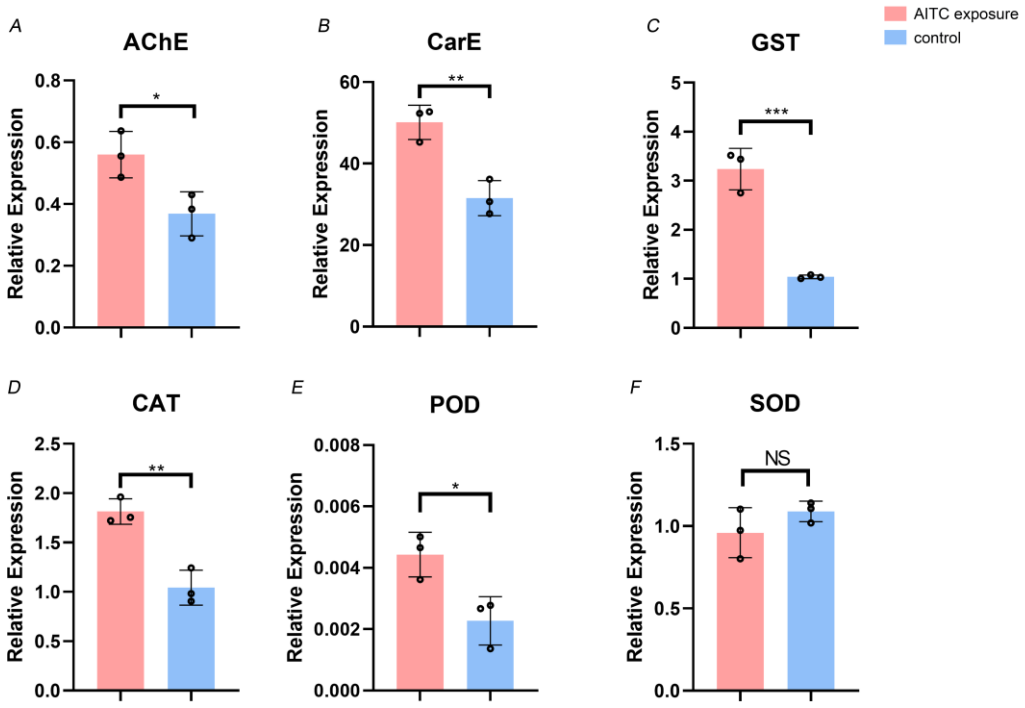

 doi:10.20944/preprints202605.1541.v1

Figure 1. Effects of the LC_{50} of AITC on enzyme activities in *C. formosanus*. Enzymatic activities were measured in termites treated with either AITC (red bar) or n-hexane (blue bar). Data are presented as the mean±SD (n=3). Statistical significance between the AITC-treated group and the control group was determined by student's *t* tests (and nonparametric tests). *$p < 0.05$, **$p < 0.01$ and ***$p < 0.001$ indicate significant difference; NS, not significant.

3.2. Comparative Phylogenetic Analysis of Key Enzymes in C. formosanus and Other Insects

In this study, we identified 20 genes encoding targeting enzymes based on CDS prediction from our previous transcriptome [29]. Phylogenetic trees were constructed to analyze the homology relationships of six functional gene families (AChE, CarE, CAT, GST, POD, and SOD) in the *C. formosanus* and other insects (e.g., *Cryptotermes secundus*, *Zootermopsis nevadensis*) (Table S1). And, we systematically named and classified the target genes based on their evolutionary relationships, providing a relatively standardized nomenclature system for related genes in *C. formosanus* (Fig. 2 A-F). The results showed that the CarE genes of *C. formosanus* were divided into two categories: venomous CarE and β-EST. The GST genes mainly belonged to the Sigma and Omega subfamilies, while the POD genes were classified into TPx and POD groups. The SOD genes clustered into an independent clade, forming a unique group distinct from those of other species. In addition, only one type of AChE and CAT gene was identified.

 doi:10.20944/preprints202605.1541.v1

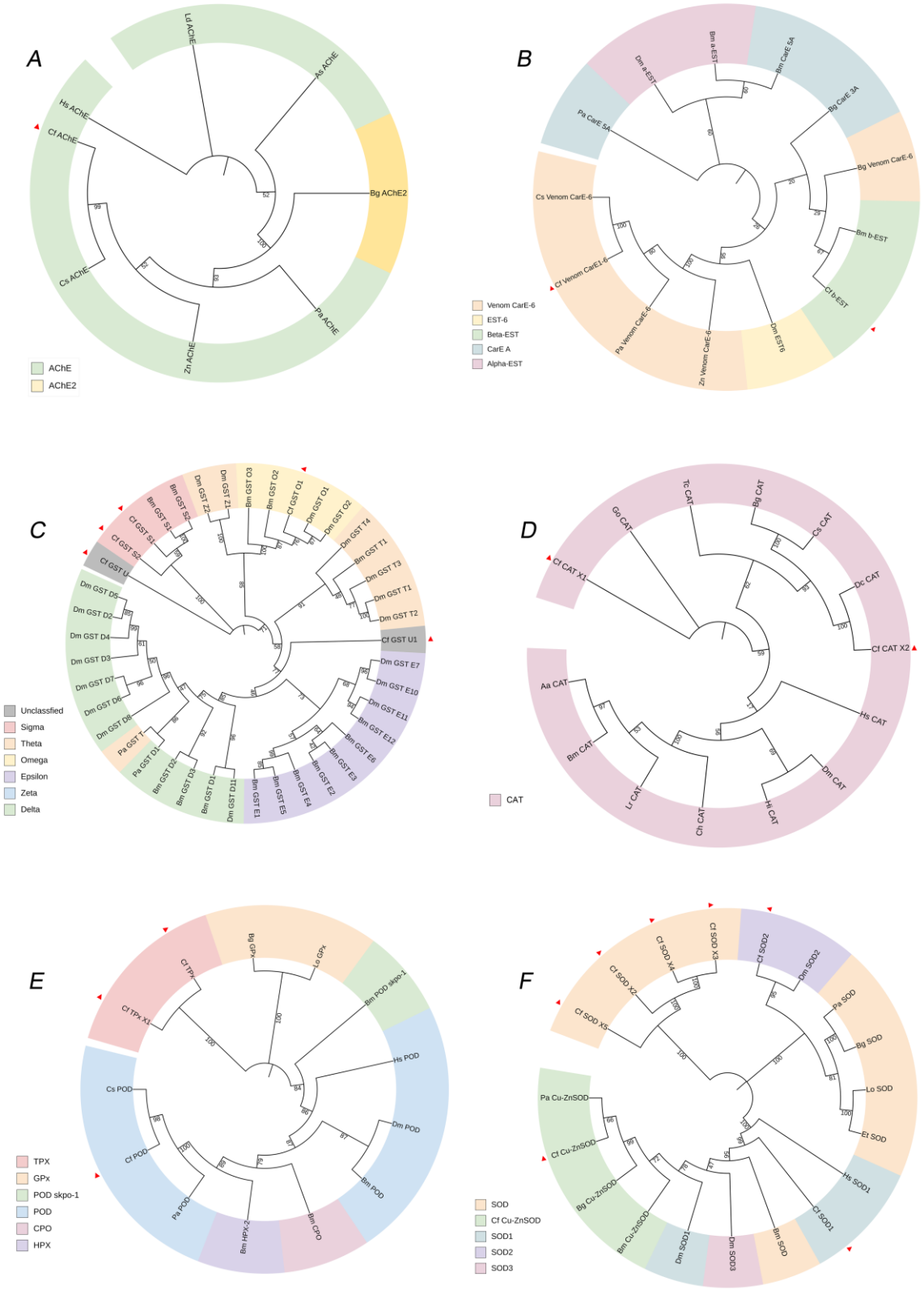

Figure 2. Phylogenetic relationships of targeting enzymes in *C. formosanus* and other insect species. Phylogenetic trees were constructed for six target gene families of *C. formosanus*: (A) AChE, (B) CarE, (C) GST, (D) CAT, (E) POD, and (F) SOD. Sequences of our *C. formosanus* (marked with red triangles) were aligned with homologous sequences from other insects (e.g., *Cryptotermes secundus, Zootermopsis nevadensis*).

 doi:10.20944/preprints202605.1541.v1

3.3. AITC Exposure at LC_{50} Enhances Gene Expression in *C. formosanus*

To elucidate the effects of AITC on the gene expression in *C. formosanus*. We determined the relative expression levels of genes encoding these enzymes in termites treated with either n-hexane (control) or a LC_{50} of AITC (Fig. 3). Among these 20 genes, 10 genes were upregulated (*Cf AChE*, *Cf b-EST*, *Cf GST O1*, *Cf GST S1*, *Cf POD*, *Cf TPx*, *Cf TPx X1*, *Cf SOD X2*, *Cf SOD X3*, *Cf SOD X4*), 4 genes were downregulated (*Cf Venom CarE-6*, *Cf GST S2*, *Cf SOD1*, *Cf SOD2*), and the remaining 6 genes showed no significant changes (*Cf GST U*, *Cf GST U1*, *Cf CAT X2*, *Cf CAT X1*, *Cf Cu-ZnSOD*, *Cf SOD X5*). Excluding the CAT family, the most highly induced genes in each enzyme family were *Cf AChE*, *Cf b-EST*, *Cf GST O1*, *Cf TPx X1*, and *Cf SOD3*. Among them, *Cf SOD3* exhibited the strongest upregulation, with its expression level increasing to 660% of the control. Notably, genes encoding GST, CarE, and SOD exhibited distinct subtype-specific expression patterns, indicating functional differentiation among different isoforms during AITC metabolism.

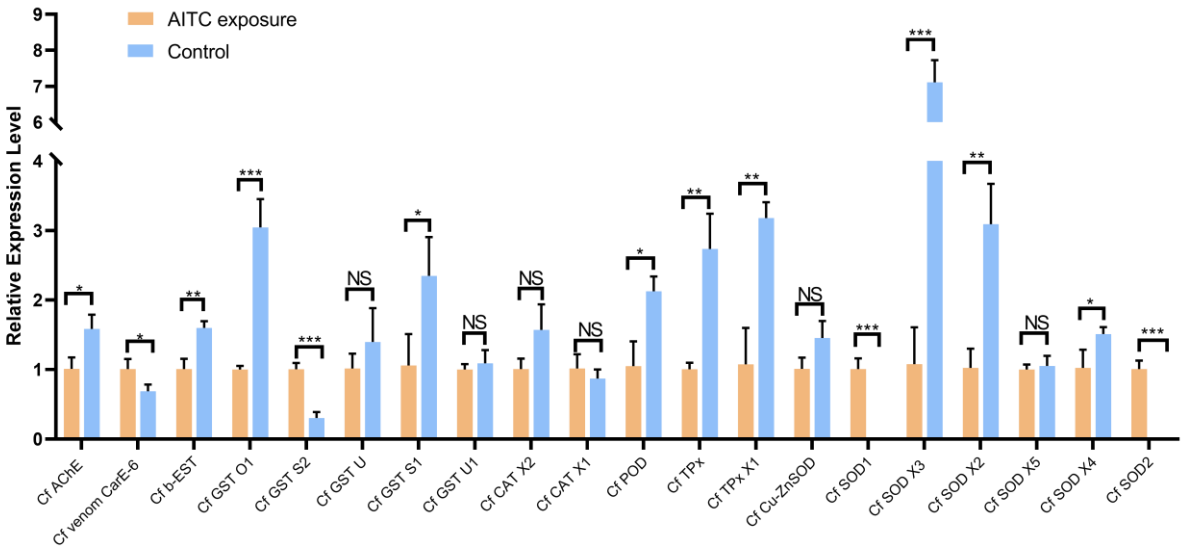

Figure 3. Effects of AITC at LC_{50} on the gene expression of target enzymes in *Coptotermes formosanus.* Enzymatic gene relative expression levels were measured in termites treated with either AITC (blue bar) or a control solution (yellow bar). Data are presented as the mean±SD (n=9). Statistical significance between the AITC-treated group and the control group was determined by Student's *t* tests (and nonparametric tests). *$p < 0.05$, **$p < 0.01$ and ***$p < 0.001$ indicate significant differences; NS, not significant.

3.4. Molecular Docking Analysis of AITC with Key Enzymes in *C. formosanus*

Based on the enzyme activity assays and gene expression results, all tested enzymes showed significant induction following AITC exposure except CAT. In particular, *Cf AChE*, *Cf b-EST*, *GSTO1*, *Cf TPx*, and *Cf SODX3*.exhibited the highest levels of induction within their respective enzyme categories. To further explore their potential roles in the response to AITC, we analyzed the interactions between AITC and these proteins by examining their predicted three-dimensional structures and binding affinities through molecular docking. The molecular docking was performed using CB-Dock2, and their binding energies were calculated. In the visualization, the interactions between AITC and specific amino acid residues of the enzyme could be observed (Fig. 4, A–E). The three-dimensional structure of AITC and its binding site within the enzyme were clearly illustrated (Fig. 4, A1–E1). From the perspective of binding energy, AITC exhibited negative binding energies with all tested enzymes (Table 1). The binding energy values increased in the order: Cf AChE < Cf GSTO1 = Cf SODX3 < Cf TPx < Cf b-EST, indicating spontaneous binding. All binding energies were

 doi:10.20944/preprints202605.1541.v1

below −1.2 kcal/mol, suggesting favorable interactions between AITC and these enzymatic targets [38].

Table 1. Docking binding energies of AITC with corresponding enzymes.

Enzyme	Vina score (kcal/mol)
Cf AChE	-3.5
Cf b-EST	-2.9
Cf GST O1	-3.4
Cf TPx	-3.2
Cf SODX3	-3.4

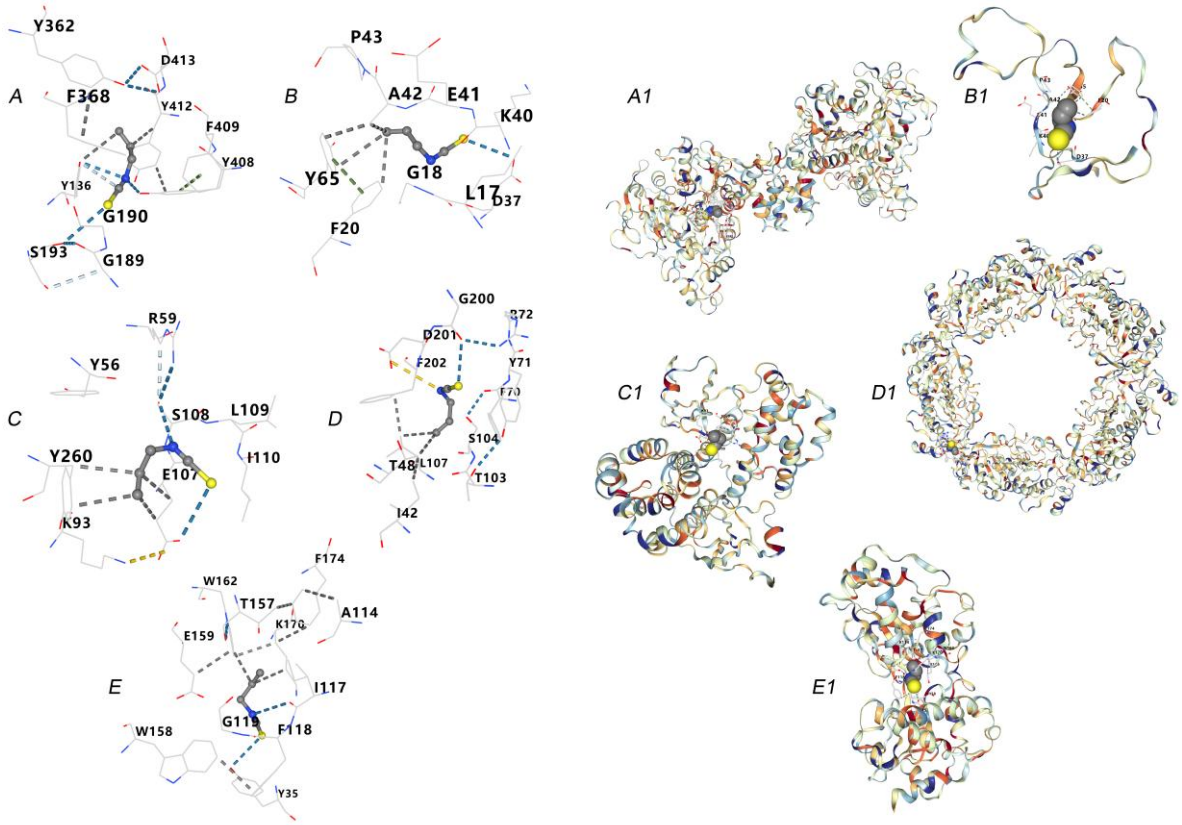

Figure 4. Molecular docking of AITC with selected target enzymes in selected target enzymes in *C. formosanus*. (Interactions with amino acid residues within the active pocket (A–E) Binding active site (A1–E1)). A: Cf AChE, B: Cf b-EST, C: GST O1, D: Cf TPx, E: Cf SODX3. The interactions between AITC and the target proteins, including hydrogen bonds (blue), weak hydrogen bonds (light blue), hydrophobic interactions (gray), and ionic interactions (yellow), pi-pi stacking (green) (A1-E1).

4. Discussion

Under adverse stress conditions, insects activate physiological defense systems, including detoxification and antioxidant systems, to maintain homeostasis [15, 16]. Among these, superoxide dismutase (SOD), peroxidase (POD), and catalase (CAT) constitute the primary protective enzyme systems, functioning coordinately to regulate reactive oxygen species (ROS) and mitigate oxidative damage. SOD catalyzes the dismutation of superoxide anion radicals to generate hydrogen peroxide (H_2O_2), which is subsequently decomposed into water and oxygen by CAT and POD, thereby maintaining cellular redox balance [39–41]. In this study, the activities of SOD, POD, and CAT were significantly elevated in the AT group compared to the CK group, indicating that AITC induced oxidative stress in *C. formosanus*. The coordinated upregulation of these enzymes suggests an

 doi:10.20944/preprints202605.1541.v1

adaptive response to increased ROS levels, helping to alleviate oxidative damage. Similar responses have been reported in other insects under insecticide stress. For instance, in *Trichogramma ostriniae*, significant increases in the activities of SOD, POD, and CAT were observed after exposure to lambda-cyhalothrin [42]. At the transcriptional level, several antioxidant-related genes, *Cf POD*, *Cf TPx*, and *Cf TPx X1* were significantly upregulated, consistent with the observed increases in enzyme activities. In contrast, *Cf CAT* genes did not show significant differences, suggesting that the elevated CAT activity may be regulated at the post-transcriptional level or enzymatic level. The expression patterns of SOD-related genes were more variable, with some isoforms upregulated and others downregulated or unchanged. Notably, several *Cf SOD* genes showed increased expression following AITC exposure, indicating their potential involvement in the oxidative stress response. These results suggest that different SOD isoforms may play distinct roles in mediating the response of *C. formosanus* to AITC. Consistent with this, molecular docking analysis showed that AITC exhibited favorable binding affinities with Cf SODX3 protein, suggesting potential interactions between AITC and SOD. Together, these findings support the involvement of SOD in the termite's response to AITC-induced stress, although the relative contribution of specific isoforms requires further investigation.

CarE and GST are key detoxification enzyme systems involved in the metabolism of xenobiotics in insects [20, 21]. In the present study, both CarE and GST activities were significantly increased following AITC exposure, indicating activation of the detoxification pathway in *C. formosanus*. The elevated GST activity suggests enhanced conjugation of toxic compounds with glutathione, facilitating their detoxification and excretion, while increased CarE activity may contribute to the hydrolysis of AITC or its derivatives. These results suggest that CarE and GST play important roles in the detoxification response of termites to AITC stress. This finding aligns with the common response patterns observed in various insect species under insecticide stress. For instance, Ruttanaphan et al. observed that sublethal concentrations of cypermethrin significantly enhanced the activities of CarEs and GSTs in field populations of *Spodoptera litura* [43]. Similarly, Li et al. reported that exposure to sublethal concentrations of abamectin, chlorpyrifos, and phoxim induced a marked increase in GST activity in *Nilaparvata lugens* [44]. At the transcriptional level, the two CarE genes (*Cf b-EST* and *Cf venomCarE-6*) showed differential expression, with *Cf b-EST* upregulated and *Cf venomCarE-6* downregulated. Despite this contrasting pattern, overall CarE enzyme activity increased, suggesting that different CarE isoforms may contribute unequally to the detoxification response and that regulation may occur beyond the transcriptional level. For GSTs, expression patterns also varied among isoforms. *Cf GSTO1* and *Cf GSTS1* were significantly upregulated, whereas *Cf GSTS2* was downregulated, and *Cf GST U* and *Cf GST U1* showed no significant change. These results indicate that GST isoforms are differentially regulated in response to AITC exposure.

Acetylcholinesterase (AChE) plays a critical role in cholinergic synaptic transmission by hydrolyzing acetylcholine (ACh), thereby terminating nerve impulses and maintaining normal neural functions [45]. In this study, AITC exposure significantly elevated AChE activity and upregulated *Cf AChE* expression in *C. formosanus*. This response may reflect a compensatory or adaptive mechanism to maintain neural homeostasis under chemical stress, rather than direct inhibition of AChE activity. Unlike classical neurotoxic insecticides that inhibit AChE, the observed increase in AChE activity suggests that AITC may not act as a typical AChE inhibitor. However, molecular docking results indicate that AITC has the potential to interact with AChE, suggesting possible modulation of enzyme function. Further biochemical and kinetic studies are needed to determine whether AITC directly affects AChE activity or indirectly influences cholinergic signaling pathways.

5. Conclusion

In summary, this study provides a comprehensive analysis of the response of *C. formosanus* to AITC at the physiological, transcriptional, protein, and molecular levels, integrating enzyme activity assays, phylogenetic characterization, gene expression analysis, and molecular docking. The results

 doi:10.20944/preprints202605.1541.v1

indicate that antioxidant and detoxification systems play important roles in the termite's response to AITC exposure. These findings offer a foundation for future studies, such as functional validation of key genes (e.g., via RNA interference) and further investigation into the interactions between AITC and target proteins. Meanwhile, the molecular docking results provide preliminary insights that may inform future optimization of AITC-based compounds. Overall, this study contributes to a better understanding of the mechanisms underlying AITC response and supports the development of environmentally friendly strategies for termite control.

Supplementary Materials: The following supporting information can be downloaded at the website of this paper posted on Preprints.org. Table S1 lists the sequences used for phylogenetic tree construction. Table S2 contains the qPCR primers.

Author Contributions: Wangyan Jiang: Writing – review & editing, Writing – original draft, Visualization, Software, Methodology, Investigation, Formal analysis, Data curation, Conceptualization. **Lijun Cai:** Funding acquisition, Visualization, Methodology, Formal analysis. **Tianyi Yang**: Visualization, Methodology, Formal analysis, Data curation. **Jiafu Zhang**: Investigation, Data curation. **Qi Zhao**: Visualization, Methodology, Data curation. **Meixiang Wu**: Funding acquisition, Writing – review & editing, Visualization, Supervision, Conceptualization.

Funding: This work was supported by the Foreign Cooperation Project of Science and Technology Department of Fujian Province (2022I0009), Test Project of Fuzhou Road Greening Maintenance and Cultivation (KH260057A).

Data Availability Statement: Data will be made available on request.

Acknowledgments: We appreciate the comments and suggestions from Fang Zhu which significantly helped improve this article.

Conflicts of Interest: The authors declare no conflicts of interest.

References

1. Hellemans, S.; Rocha, M. M.; Wang, M.; Romero Arias, J.; Aanen, D. K.; Bagnères, A. G.; Buček, A.; Carrijo, T. F.; Chouvenc, T.; Cuezzo, C.; Constantini, J. P.; et al. Genomic data provide insights into the classification of extant termites. *Nat. Commun.* **2024**, *15*, 6724. https://doi.org/10.1038/s41467-024-51028-y.
2. Chouvenc, T.; Sobotnik, J.; Engel, M. S.; Bourguignon, T. Termite evolution: mutualistic associations, key innovations, and the rise of Termitidae. *Cell. Mol. Life Sci.* **2021**, *78*, 2749–2769. https://doi.org/10.1007/s00018-020-03728-z
3. Gazdick, K.; Lee, S.-B.; Mizumoto, N.; Chouvenc, T.; Su, N.-Y. Subterranean termites (*Coptotermes formosanus* [Blattodea: Rhinotermitidae]) colonies can readily intercept commercial in-ground bait stations placed at label-prescribed distance. *J. Econ. Entomol.* **2025**, *118*, 1363–1372. https://doi.org/10.1093/jee/toae259
4. Cao, R.; Feng, J. Future climate change and anthropogenic disturbance promote the invasions of the world's worst invasive insect pests. *Insects.* **2024**, *15*, 280. https://doi.org/10.3390/insects15040280
5. Oi, F. A review of the evolution of termite control: A continuum of alternatives to termiticides in the United States with emphasis on efficacy testing requirements for product registration. *Insects.* **2022**, *13*, 50. https://doi.org/10.3390/insects13010050
6. Isman, M. B. Bioinsecticides based on plant essential oils: a short overview. *Z. Naturforsch. C.* **2020**, *75*, 179–182. https://doi.org/10.1515/znc-2020-0038
7. Cheng, S. S.; Lin, C. Y.; Chen, Y. J.; Chung, M. J.; Chang, S. T. Insecticidal activities of *Cunninghamia konishii* Hayata against Formosan subterranean termite, *Coptotermes formosanus* (Isoptera: Rhinotermitidae). *Pest Manage. Sci.* **2014**, *70*, 1215–1219. https://doi.org/10.1002/ps.3673
8. Cheng, S. S.; Lin, C. Y.; Chung, M. J.; Chang, S. T. Chemical composition and antitermitic activity against *Coptotermes formosanus* Shiraki of *Cryptomeria japonica* leaf essential oil. *Chem. Biodivers.* **2012**, *9*, 352–358. https://doi.org/10.1002/cbdv.201100243

 doi:10.20944/preprints202605.1541.v1

9. Pornpun, S.; Ohtani, Y.; Ichiura, H. Biological performance of *Eucalyptus camaldulensis* leaf oils from Thailand against the subterranean termite *Coptotermes formosanus* Shiraki. J. *Wood Sci.* **2009**, *55*, 41–46. https://doi.org/10.1007/s10086-008-0990-4
10. Bahmid, N. A.; Heising, J.; Dekker, M. Multiresponse kinetic modelling of the formation, release, and degradation of allyl isothiocyanate from ground mustard seeds to improve active packaging. *J. Food Eng.* **2021**, *292*, 110370. https://doi.org/10.1016/j.jfoodeng.2020.110370
11. Mansour, E. E.; Mi, F.; Zhang, G.; Xie, J.; Wang, Y.; Kargbo, A. Effect of allyl isothiocyanate on *Sitophilus oryzae*, *Tribolium confusum* and *Plodia interpunctella*: Toxicity and effect on insect mitochondria. *Crop Prot*. **2012**, *33*, 40–51. https://doi.org/10.1016/j.cropro.2011.11.010
12. Guo, Y. P.; Quandahor, P.; Mao, L.; Li, C. C.; Zhou, J. J.; Liu, C. Z. Responses of fungi maggot (*Bradysia impatiens* Johannsen) to allyl isothiocyanate and high CO_2. *Front. Physiol.* **2022**, *13*, 879401. https://doi.org/10.3389/fphys.2022.879401
13. Du, Y.; Grodowitz, M. J.; Chen, J. Insecticidal and enzyme inhibitory activities of isothiocyanates against red imported fire ants, *Solenopsis invicta*. *Biomolecules*. **2020**, *10*, 716. https://doi.org/10.3390/biom10050716
14. Jiang, L.; Li, Y.; Shi, W.; Chen, W.; Ma, Z.; Feng, J.; Hashem, A. S.; Wu, H. Cloning and expression of the mitochondrial cytochrome c oxidase subunit II gene in *Sitophilus zeamais* and interaction mechanism with allyl isothiocyanate. *Pestic. Biochem. Physiol.* **2023**, *192*, 105392. https://doi.org/10.1016/j.pestbp.2023.105392
15. Felton, G.; Summers, C.B. Antioxidant systems in insects. *Arch. Insect Biochem. Physiol.* **1995**, *29*, 187–197. https://doi.org/10.1002/arch.940290208
16. Corona, M.; Robinson, G.E. Genes of the antioxidant system of the honey bee: annotation and phylogeny. *Insect Mol. Biol.* **2006**, *15*, 687–701. https://doi.org/ 10.1111/j.1365-2583.2006.00695.x
17. Liu, Y.; Zhu, F.; Shen, Z.; Moural, T. W.; Liu, L.; Li, Z.; Liu, X.; Xu, H. Glutaredoxins and thioredoxin peroxidase involved in defense of emamectin benzoate induced oxidative stress in *Grapholita molesta*. *Pestic. Biochem. Physiol.* **2021,** *176*, 104881. https://doi.org/ 10.1016/j.pestbp.2021.104881
18. Feyereisen R. Insect CYP genes and P450 enzymes. In: Gilbert LI, ed. Insect Molecular Biology and Biochemistry. San Diego: Academic Press, **2012**, 236–316.
19. Nauen R.; Bass C.; Feyereisen R.; Vontas J. The role of cytochrome P450s in insect toxicology and resistance. *Annu. Rev. Entomol.* **2022**, *67*, 105–124. https://doi.org/ 10.1146/annurev-ento-070621-061328
20. Cruse C.; Moural T. W.; Zhu F. Dynamic roles of insect carboxyl/cholinesterases in chemical adaptation. *Insects.* **2023**, *14*, 194. https://doi.org/ 10.3390/insects14020194
21. Koirala B K S.; Moural T. W.; Zhu F. Functional and structural diversity of insect glutathione S-transferases in xenobiotic adaptation. *Int. J. Biol. Sci.* **2022**, *18*, 5713–5723. https://doi.org/ 10.7150/ijbs.77141
22. Casida, J. E.; Durkin, K. A. Anticholinesterase insecticide retrospective. *Chem. Res. Toxicol.* **2013**, *26*, 114–125. https://doi.org/ 10.1016/j.cbi.2012.08.002
23. Sledz, P.; Caflisch, A. Protein structure-based drug design: from docking to molecular dynamics. *Curr. Opin. Struct. Biol.* **2018**, *48*, 93–102. https://doi.org/10.1016/j.sbi.2017.10.010
24. Smach, M. A.; Hafsa, J.; Ben Abdallah, J.; Charfeddine, B.; Limem, K. Neuroprotective and anti-amnesic effects of *Laurus Nobilis* essential oil against scopolamine-induced memory deficits in mice brain. *J. Ethnopharmacol.* **2024**, *319* Pt 1, 117151. https://doi.org/10.1016/j.jep.2023.117151
25. Hazarika, M.; Nath, P.; Begum, T.; Lal, M.; Kalita, J.; Dutta, P. Insights into insecticidal efficacy of *Cymbopogon* essential oils against *Callosobruchus chinensis*: An integrated approach through bioassays and in-silico molecular docking for sustainable pest management. *J. Stored Prod. Res.* **2025**, *112*, 102655. https://doi.org/10.1016/j.jspr.2025.102655
26. Arya, S.; Kumar, R.; Karakoti, H.; Mahawer, S. K.; Prakash, O.; Kumar, S.; Latwal, M.; Panday, G.; de Oliveira, M. S. Seasonal study chemical profiles and bioactivities of *Hedychium coronarium* J. Koenig essential oils: Nematicidal, insecticidal, phytotoxic, antifungal potentials, and molecular docking insights. *Chem. Biodivers.* **2025**, *22*, e202402160. https://doi.org/10.1002/cbdv.202402160
27. Liu, Y.; Grimm, M.; Dai, W. T.; Hou, M. C.; Xiao, Z. X.; Cao, Y. CB-Dock: a web server for cavity detection-guided protein-ligand blind docking. *Acta Pharmacol. Sin.* **2020**, *41*, 138–144. https://doi.org/10.1038/s41401-019-0228-6

 doi:10.20944/preprints202605.1541.v1

28. Liu, Y.; Yang, X.; Gan, J.; Chen, S.; Xiao, Z. X.; Cao, Y. CB-Dock2: Improved protein ligand blind docking by integrating cavity detection, docking and homologous template fitting. *Nucleic Acids Res*. **2022**, *50*, W159–W164. https://doi.org/10.1093/nar/gkac394
29. Jiang, W.; Yang, T.; Zhang, J.; Jing, H.; Huang, D.; Zheng, J.; Guo, Y.; Xu, W.; Cai, L.; Wu, M. Multi-omics reveals allyl isothiocyanate disrupts lipid metabolism, neural signaling, and glucose metabolism in *Coptotermes formosanus* (Blattodea: Heterotermitidae). *J. Econ. Entomol.* **2025**, https://doi.org/2026, 10.1093/jee/toag096
30. Camacho, C.; Coulouris, G.; Avagyan, V.; Ma, N.; Papadopoulos, J.; Bealer, K.; Madden, T. L. BLAST+: architecture and applications. *BMC Bioinf.* **2009**, *10*, 421. https://doi.org/10.1186/1471-2105-10-421
31. Tamura K.; Stecher G.; and Kumar S. MEGA11 bolecular evolutionary genetics analysis version 11. *Mol. Biol. Evol.* **2021**, *38*, 3022–3027. https://doi.org/0.1093/molbev/msab120
32. Saitou N. and Nei M. The neighbor-joining method: A new method for reconstructing phylogenetic trees. *Mol. Biol. Evol.* **1987**, *4*, 406–425. https://doi.org/ 10.1093/oxfordjournals.molbev.a040454
33. Felsenstein J. Confidence limits on phylogenies: An approach using the bootstrap. *Evolution* **1985** *39*, 783–791. https://doi.org/ 10.1111/j.1558-5646.1985.tb00420.x
34. Nei M. and Kumar S. Molecular evolution and phylogenetics. New York: Oxford University Press, **2000**.
35. Tarver, M. R.; Mattison, C. P.; Florane, C. B.; Hinchliffe, D. J.; Zhang, D.; Lax, A. R. Screening of multiple potential control genes for use in caste and body region comparisons using RT-qPCR in *Coptotermes formosanus*. *Sociobiology.* **2022**, *59*, 81–95. https://doi.org/10.13102/sociobiology.v59i1.669
36. Livak, K. J.; Schmittgen, T. D. Analysis of relative gene expression data using real-time quantitative PCR and the 2(-Delta Delta C(T)) Method. *Methods*. **2001**, *25*, 402–408. https://doi.org/10.1006/meth.2001.1262
37. Waterhouse, A.; Bertoni, M.; Bienert, S.; Studer, G.; Tauriello, G.; Gumienny, R.; Heer, FT.; de Beer, TAP.; Rempfer, C.; Bordoli, L.; Lepore, R.; Schwede, T. SWISS-MODEL: homology modelling of protein structures and complexes. *Nucleic Acids Res.* **2018**, *46*, W296–W303. https://doi.org/10.1093/nar/gky427
38. Duan, H.; Khan, GJ.; Shang, LJ.; Peng, H.; Hu, WC.; Zhang, JY.; Hua, J.; Cassandra, A.; Rashed, MMA.; Zhai, KF. Computational pharmacology and bioinformatics to explore the potential mechanism of Schisandra against atherosclerosis. *Food Chem. Toxicol*. **2021**, *150*, 112058. https://doi.org/ 10.1016/j.fct.2021.112058.
39. Lopez-Martinez, G.; Elnitsky, M. A.; Benoit, J. B.; Lee, R. E.; Denlinger, D. L. High resistance to oxidative damage in the Antarctic midge *Belgica antarctica*, and developmentally linked expression of genes encoding superoxide dismutase, catalase and heat shock proteins. *Insect Biochem. Mol. Biol.* **2008**, *38*, 796–804. https://doi.org/10.1016/10.1016/j.ibmb.2008.05.006
40. Krishnan, N.; Kodrik, D. Antioxidant enzymes in *Spodoptera littoralis* Boisduval: Are they enhanced to protect gut tissues during oxidative stress? *J. Insect Physiol.* **2006**, *52*, 11–20. https://doi.org/10.1016/j.jinsphys.2005.08.009
41. Zhu-Salzman, K.; Zeng, R. S. Insect response to plant defensive protease inhibitors. *Annu. Rev. Entomol.* **2015**, *60*, 233–252. https://doi.org/10.1146/annurev-ento-010814-020816
42. Zhu, W.; Fan, R.; Liu, M.; Wang, J.; Zhang, Y.; Ma, R. Toxic effects of five insecticides on the development and enzymatic activities of *Trichogramma ostriniae*. *J. Appl. Entomol.* **2025**, *149*, 56–64. https://doi.org/10.1111/jen.13357
43. Ruttanaphan, T.; Pluempanupat, W.; Bullangpoti, V. Cypermethrin resistance in *Spodoptera litura* Fabricius (Lepidoptera: Noctuidae) from three locations in Thailand and detoxification enzyme activities. *Agric. Nat. Resour*. **2018**, *52*, 484–488. https://doi.org/10.1016/j.anres.2018.10.014

 doi:10.20944/preprints202605.1541.v1

44. Li, G. Y.; Wu, Y.; Liu, Y. Y.; Chen, X. S. Insecticides resistance and detoxification enzymes activity changes in brown planthopper, *Nilaparvata lugens* in Guizhou Province. *Acta Ecol. Sin.* **2019**, *39*, 234–241. https://doi.org/10.1016/j.chnaes.2018.09.001
45. Fan, Y. J.; Dong, X. Y.; Yang, D.; Qin, Y.; Hu, X. P.; Zhou, H. X. New mutations of acetylcholinesterase in *Bactrocera dorsalis* populations across southern China and impact on resistance to organophosphate. *Ecotoxicol. Environ. Saf.* **2025**, *297*, 118189. https://doi.org/ 10.1016/j.ecoenv.2025.118189.